

## Cooper minima and Young-type interferences in photoionization of one-electron molecular ions

R. Della Picca, P. D. Fainstein,<sup>\*</sup> and M. L. Martiarena*Centro Atómico Bariloche, Comisión Nacional de Energía Atómica, Avda E. Bustillo 9500, 8400 Bariloche, Argentina*

N. Sisourat and A. Dubois

*Laboratoire de Chimie Physique-Matière et Rayonnement, UPMC Université Paris 06, UMR 7614, 75231 Paris Cedex 05, France  
and CNRS, UMR 7614, LCPMR, 75231 Paris Cedex 05, France*

(Received 30 July 2008; published 4 March 2009)

We study photon- and ion-induced electron emission from one-electron diatomic molecular ions. For photon impact we find an oscillatory behavior of the asymmetry parameter  $\beta$  and of the total cross section which can be related to the presence of Cooper minima in the partial cross sections. This behavior can also be related to coherent electron emission from the two centers of the molecule. By comparing the results for homonuclear and heteronuclear molecular ions, we show that the periodic structures predicted by both pictures appear clearly only for the former targets. This conclusion is supported by study of the electron emission spectra induced by swift ion impact.

DOI: [10.1103/PhysRevA.79.032702](https://doi.org/10.1103/PhysRevA.79.032702)

PACS number(s): 34.80.-i, 33.80.-b

## I. INTRODUCTION

The discovery of periodic oscillations in the electron emission spectra of  $H_2$  induced by ion impact [1] sparked an intense activity to characterize and explain the process. It was shown that these oscillations were due to the two-center character of the target and that therefore it could be explained as due to the Young-type interference of coherent waves emitted from the two centers in the molecule [2,3]. These studies were quickly extended for other projectiles, namely, electrons [4,5] and photons [6], and similar features were found in all cases.

In fact this effect was first studied by Cohen and Fano who predicted the oscillatory behavior of the electron emission spectra in photoionization of  $H_2^+$  [7]. In their pioneering work, these authors noted that the oscillations are also connected to the onset of transitions to states of increasing orbital angular momentum  $\ell$  as the electron energy increases, in opposition to the case of atomic targets where only the  $\Delta\ell = \pm 1$  terms contribute. The contributions of the  $\ell$  partial cross sections add to yield a modulating function which is essentially a function of the product  $k_e R$ , where  $k_e$  is the ejected electron momentum and  $R$  the internuclear distance. More accurate calculations performed recently by Fojón and co-workers [8] confirm this partial cross section analysis. This work also shows that the results from [7] disagree with exact calculations because of the simple initial and final state wave functions employed in the early calculations. The same kind of phenomenon was found in a recent study of inner-shell photoionization of  $N_2$  molecules [9,10]. In this case the cross-section ratio between the  $1\sigma_g$  and  $1\sigma_u$  initial states shows Young-type modulations due to the coherent emission from the two molecular centers which are also connected to the onset of transitions to states with higher  $\ell$  values.

Very recently we have presented a study of the partial cross sections as a function of photoelectron momentum for

photoionization of  $H_2^+$  [11]. The partial cross sections have minima which are known as Cooper minima and which were shown to correspond to a zero in the transition matrix, that is, to zero absorption. The Cooper minima appear at higher values of the photoelectron momentum as the angular momentum  $\ell$  increases. The interplay between the drop in the contribution from a certain  $\ell$  partial cross section and the increase of the following one produces the interference modulation discovered by Cohen and Fano.

Therefore there is an intimate relationship between Young-type interference phenomena and Cooper minima. This fact is somewhat puzzling because Cooper minima appear in the photoelectron spectra of homonuclear and heteronuclear molecular targets [12] while Young-type interference modulations are observed only in the case of homonuclear diatomic molecules ( $H_2^+$ ,  $H_2$ ,  $N_2$ , ...) in which the two "slits" are equal [13].

For atomic targets, Cooper minima appear only when the initial state has a node. For a certain photoelectron energy the transition matrix can become equal to zero because the positive and negative contributions in the integration required to evaluate the matrix elements cancel out [12,14]. In our recent work we showed that a similar effect appears for molecules when the initial state has no node, as in  $H_2^+$  [11]. Because these structures correspond to no absorption we call them "Cooper minima."

In the present work we consider the photoionization of two one-electron diatomic molecules:  $H_2^+$  and  $HeH^{2+}$ . In this way we consider the cases in which the two slits are, respectively, equal and different. Through the detailed analysis of the Cooper minima we show why, as expected, the former presents interference modulations in the cross section while the latter does not. Atomic units will be used except when otherwise stated.

## II. THEORY

We consider the photoionization of a one-electron diatomic molecule by linearly polarized light. The nuclei of the

<sup>\*</sup>pablof@cab.cnea.gov.ar

molecule have charge  $Z_a$  and  $Z_b$  and are fixed at the internuclear distance  $R$ . Employing spheroidal coordinates and using standard computational methods we calculate exactly the initial ground [15] and final continuum [16,17] states of the molecule. With these initial and final wave functions the transition matrix is evaluated numerically so that the differential cross sections are obtained for the fixed-in-space molecule as a function of the photoelectron energy and angle:

$$\frac{d\sigma}{d\hat{R}d\hat{k}_e} = 4\pi^2\alpha\omega k_e |T_{if}|^2, \quad (1)$$

where  $\mathbf{k}_e \equiv \{k_e, \theta_e, \phi_e\}$  ( $\hat{\mathbf{k}}_e = \mathbf{k}_e/k_e$ ) is the ejected electron momentum in the molecular frame,  $\hat{R} \equiv \{\Theta_R, \Phi_R\}$  the orientation of the molecule in the laboratory reference frame (defined by the radiation field),  $\alpha$  the fine structure constant, and  $\hbar\omega$  the photon energy. The transition matrix  $T_{if}$  is given by

$$T_{if} = \frac{1}{\sqrt{k}} \sum_{m\ell} (-i)^\ell e^{i\Delta_{m\ell}} \mathcal{Y}_{\ell m}(c, \theta_e, \phi_e) M_{\ell m}, \quad (2)$$

where  $\Delta_{m\ell}$  is the phase shift,  $\mathcal{Y}_{\ell m}$  the spheroidal harmonics,  $c = k_e R/2$ , and

$$M_{\ell m} = \langle \psi_{mq}^{(-)}(\mathbf{k}_e, \mathbf{r}) | \hat{\mathbf{e}} \cdot \mathbf{D} | \psi_i(\mathbf{r}) \rangle \quad (3)$$

with  $E_e = k_e^2/2$  the photoelectron energy. The functions  $\psi_i(\mathbf{r})$  and  $\psi_{mq}^{(-)}(\mathbf{k}_e, \mathbf{r})$ , with  $\ell = q + m$ , are the initial and final exact wave functions with correct asymptotic conditions for the latter. The dipole operator  $\mathbf{D}$  in Eq. (3) is given by  $\mathbf{D} = \nabla/\omega$  or  $\mathbf{D} = \mathbf{r}$  in the velocity and length gauges, respectively. The differential cross section can be integrated over the orientation of the molecule and the emission angle of the photoelectron to get the total cross section. We have calculated these quantities to compare with the ones obtained previously with similar methods by Richards and Larkins [18], and detailed checks were also performed using the velocity and length gauges. Perfect agreement was found in all cases (see [11] for details). Within the Born-Oppenheimer and dipolar approximations our calculations can be considered as exact.

After averaging over the molecular orientation, the differential cross section for a randomly oriented molecular target can be cast in the form [18]

$$\frac{d\sigma}{d\Omega} = \frac{\sigma_{\text{tot}}}{4\pi} [1 + \beta P_2(\cos \theta)] \quad (4)$$

with  $\sigma_{\text{tot}}$  the total cross section,  $\theta$  the photoelectron ejection angle with respect to the polarization vector, and  $P_2(\cos \theta) = \frac{1}{2}(3 \cos^2 \theta - 1)$  the second-order Legendre polynomial. The asymmetry parameter  $\beta$ , which varies in the range  $-1 \leq \beta \leq 2$ , determines completely the angular distribution of the photoelectrons. The value  $\beta = 2$  corresponds to the atomic target case, which can be obtained either in the united atom limit or in the molecular case at asymptotic high photoelectron energies.

The matrix element given in Eq. (3) corresponds to transitions to final states with angular momentum  $\ell$  and projection  $m$  onto the internuclear axis. Due to the symmetries of the initial ground state and the dipolar operator, the projec-

tion of the angular momentum operator  $m$  can take only the values 0 ( $\sigma \rightarrow \sigma$ ) and  $\pm 1$  ( $\sigma \rightarrow \pi$ ). Moreover, for parallel alignment between the internuclear and the polarization vectors only  $\sigma \rightarrow \sigma$  transitions can occur, while for the perpendicular arrangement only  $\sigma \rightarrow \pi$  transitions are allowed. The total cross section can then be calculated as

$$\sigma_{\text{tot}} = \sigma_\sigma + 2\sigma_\pi, \quad (5)$$

where the total cross sections  $\sigma_\sigma$  and  $\sigma_\pi$  for  $\sigma \rightarrow \sigma$  and  $\sigma \rightarrow \pi$  transitions, respectively, are given by

$$\sigma_\sigma = \sum_\ell \sigma_{\ell 0}, \quad (6)$$

$$\sigma_\pi = \sum_\ell \sigma_{\ell 1}, \quad (7)$$

with

$$\sigma_{\ell m} = \frac{4\pi^2\alpha}{3\omega} |\mathcal{M}_{\ell m}|^2, \quad (8)$$

where  $\mathcal{M}_{\ell m}$  are reduced matrix elements [see Eq. (7) in [11]]. For homonuclear molecules, like  $\text{H}_2^+$ , the angular momentum quantum number  $\ell$  can take only odd values. This selection rule does not apply for heteronuclear molecules. In the following we will see how this fundamental difference is related to the appearance or not of interference modulations. Moreover, we will concentrate our analysis on  $(\sigma_{\ell 0}, \sigma_\sigma)$  because for  $(\sigma_{\ell 1}, \sigma_\pi)$  a similar effect is not observed (see, for example, the results in Table 1 of [18] and Fig. 2 in [19]).

### III. RESULTS AND DISCUSSION

#### A. Homonuclear molecular targets: The $\text{H}_2^+$ case

We first calculate the asymmetry parameter  $\beta$  for  $\text{H}_2^+$  at the equilibrium internuclear distance  $R = 2$  a.u.: the results are presented in Fig. 1(b) in comparison with previous data from [18]. As expected, the  $\beta$  parameter seems to increase as the photoelectron momentum increases, tending to the limiting value of 2 which corresponds to the atomic target case. In Fig. 1(a), we present a magnification of these data especially focused on high photoelectron energies, where a periodic oscillation of small amplitude can be observed. If we now compare with the partial cross sections  $\sigma_{\ell 0}$ , shown in Fig. 1(c), we notice that the Cooper minima of the different partial waves are directly related to the oscillations since the minima in the oscillations of  $\beta$  appear at the position of the Cooper minima. Moreover, we notice that the cross section  $\sigma_\sigma$  (solid line with + sign) also oscillates in phase with  $\beta$ .

This is a general feature of the process: the asymmetry parameter  $\beta$  for the internuclear distance  $R = 3$  a.u., presented in Fig. 2, shows again a periodic oscillatory behavior with minima located for electron momenta  $k_e$  corresponding to the Cooper minima. As  $R$  increases, the Cooper minima for the different  $\ell$  values move closer to each other and thus the frequency of the oscillations increases. This result is in agreement with a recent work by Fernández *et al.* [19], in which the minima for each  $\ell$  partial cross section were shown to appear for electron wave vectors  $k_e(\ell)$  satisfying

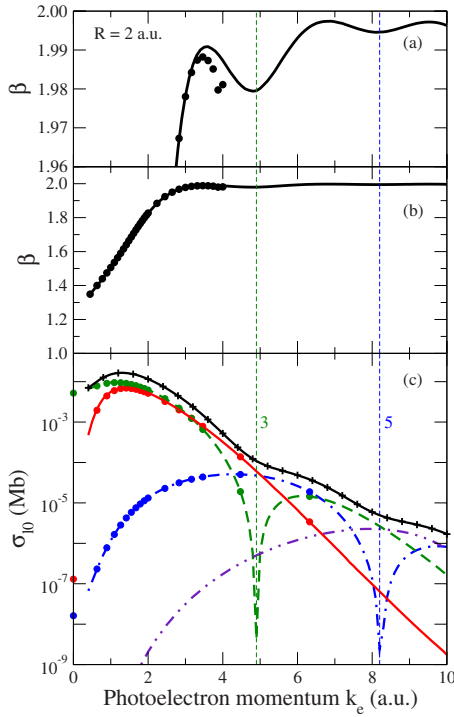


FIG. 1. (Color online) Photoionization of  $H_2^+$  with  $R=2$  a.u. (a) Asymmetry parameter  $\beta$ : solid line, present results; circles, from [18]. (b) Asymmetry parameter  $\beta$ : solid line, present results; circles, from [18]. (c) Partial cross sections  $\sigma_{\ell 0}$ : solid line with + sign, total cross section  $\sigma_\sigma$ ; solid line,  $\sigma_{10}$ ; dashed line,  $\sigma_{30}$ ; dotted-dashed line,  $\sigma_{50}$ ; double-dotted-dashed line,  $\sigma_{70}$ ; circles, from [18]. The numbers in (c) indicate the  $\ell$  value corresponding to the Cooper minima. The vertical dashed lines indicate the positions of the Cooper minima in each partial cross section.

the relationship  $k_e(\ell)R \sim \ell\pi$ . Therefore, the wavelength of the oscillation, which is simply  $k_e(\ell+2) - k_e(\ell)$ , decreases with increasing  $R$  and thus the frequency increases linearly with the internuclear distance  $R$ .

It has been known for some time that the Cooper minima in photoionization of excited states produce large variations on the angular distributions [12,20,21]. For example, measurements and calculations in photoionization of HCl show that  $\beta$  does not rise continuously but has a minimum at the value where a Cooper minimum appears (see [20] and references therein). Our present results show unexpectedly that there are periodic oscillations in  $\beta$  in photoionization of the  $1s\sigma$  state of  $H_2^+$ . From our calculations of  $\beta$ , shown in Figs. 1 and 2, we see that, contrary to what was found for HCl, the amplitude of the oscillations is very small and probably that is the reason why they were undetected until now.

To analyze in more detail the relation between the Cooper minima and the oscillations in  $\beta$ , we employ a partitioning scheme for the asymmetry parameter introduced by Thiel [22]. For the present case, it can be written as

$$\beta = \beta_{\sigma\sigma} + \beta_{\sigma\pi} + \beta_{\pi\pi}, \quad (9)$$

where  $\beta_{\sigma\sigma}$  and  $\beta_{\pi\pi}$  are intrachannel contributions and  $\beta_{\sigma\pi}$  the interchannel contribution. The results for  $\beta$  with  $R = 2$  a.u. are shown in Fig. 3(a) and the different contributions in Fig. 3(b). It can be seen that the  $\beta_{\sigma\sigma}$  intrachannel con-

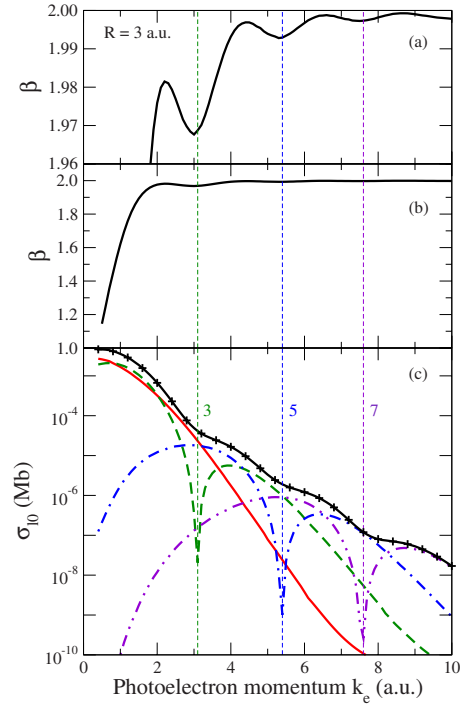


FIG. 2. (Color online) Same as Fig. 1 but for  $R=3$  a.u.

tribution is in phase with  $\beta$ , confirming therefore the close relationship between the oscillations in the asymmetry parameter and the Cooper minima, which appear only in  $\sigma \rightarrow \sigma$  transitions. The other two contributions, which include  $\sigma \rightarrow \pi$  transitions, do not show any clear coherence with  $\beta$ . However, their sum labeled as  $\beta_\pi$  has a phase difference of  $\pi/2$  with  $\beta_{\sigma\sigma}$ . The amplitude of this last contribution is slightly larger than that of  $\beta_\pi$ , and that is the reason why both oscillations do not exactly cancel, giving rise to a small

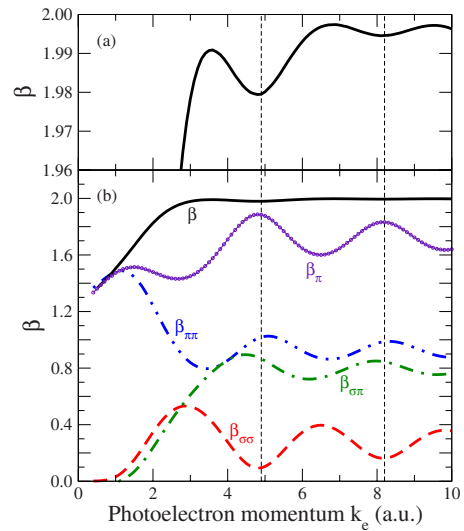


FIG. 3. (Color online) Photoionization of  $H_2^+$  with  $R=2$  a.u. (a) Asymmetry parameter  $\beta$ : solid line, present results; circles, from [18]. (b) Asymmetry parameter  $\beta$ : solid line, present results; circles, from [18]. (c) Partial cross sections  $\sigma_{\ell 0}$ : solid line with + sign, total cross section  $\sigma_\sigma$ ; solid line,  $\sigma_{10}$ ; dashed line,  $\sigma_{30}$ ; dotted-dashed line,  $\sigma_{50}$ ; double-dotted-dashed line,  $\sigma_{70}$ ; circles, from [18]. The numbers in (c) indicate the  $\ell$  value corresponding to the Cooper minima. The vertical dashed lines indicate the positions of the Cooper minima in each partial cross section.

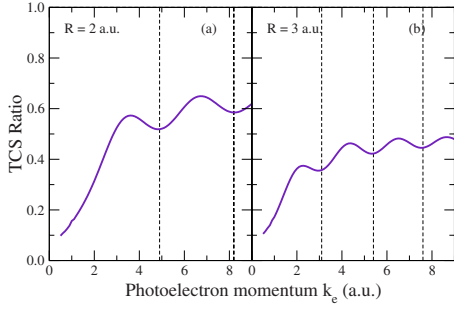


FIG. 4. (Color online) Ratio between the photoionization total cross section for  $\text{H}_2^+$  and H (multiplied by 2).  $R = (a)$  2 and  $(b)$  3 a.u. The vertical dashed lines indicate the positions of the Cooper minima in the partial cross sections.

modulation in  $\beta$ , in phase with  $\beta_{\sigma\sigma}$ . For  $R=3$  a.u. the same behavior is also found.

As seen in Figs. 1 and 2 the oscillations in  $\beta$  are small and thus difficult to observe experimentally. We present therefore in Fig. 4 the ratio between the total photoionization cross sections for  $\text{H}_2^+$  (at  $R=2$  and 3 a.u.) and the ones for a H atom (multiplied by 2). The two ratios present the oscillations attributed to coherent electron emission by Cohen and Fano [7], the minima of which coincide with the position of the Cooper minima (shown as vertical dashed lines). It results therefore that there is a close relationship between the Cooper minima and the periodic oscillations both in  $\beta$  and in the total cross-section ratio. It remains to see how the Cooper minima are related to the coherent electron emission responsible for the Young-type interference modulations. For this purpose we analyze the case of a one-electron heteronuclear molecular target.

### B. Heteronuclear molecular targets: The $\text{HeH}^{2+}$ case

In Sec. III A we have analyzed the relationship between Cooper minima and the oscillations in the asymmetry parameter and the total cross sections for homonuclear molecules. We now consider the case of a heteronuclear molecular target, where it can be expected, in analogy with Young's double-slit experiment, that no clear interference pattern will arise, as the two slits are different.

For this purpose we consider the heteronuclear one-electron  $\text{HeH}^{2+}$  molecule. We first performed the calculations for the repulsive  $1s\sigma$  initial state at an internuclear distance  $R=2$  a.u. One of the important differences between the processes of photoionization of  $\text{HeH}^{2+}$  and  $\text{H}_2^+$  is that for the former there is no selection rule for the angular momentum so that amplitudes with even and odd values of  $\ell$  contribute to the total cross section and asymmetry parameter. As can be seen in Figs. 5(a) and 5(b),  $\beta$  increases monotonically up to the limiting value of 2 and present some structures, though extremely weak in magnitude. However the  $\sigma_\sigma$  cross sections [solid line with + sign in Fig. 5(c)] show no structure, contrary to what was obtained for  $\text{H}_2^+$ . In summary, the  $\beta$  parameter and  $\sigma_\sigma$  cross section do not show clear oscillations, in agreement with what would be expected from Young-type interference effects, even though, as can be seen in Fig. 5(c),

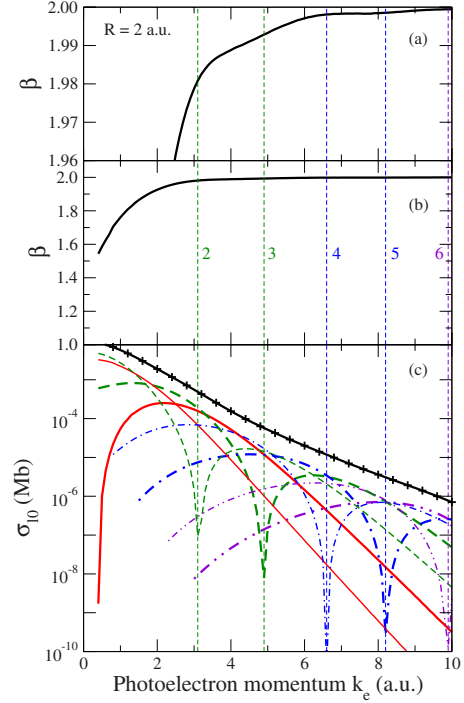


FIG. 5. (Color online) Photoionization of  $\text{HeH}^{2+}$  in the  $1s\sigma$  initial state with  $R=2$  a.u. (a), (b) Asymmetry parameter  $\beta$ . The numbers in (b) indicate the  $\ell$  values corresponding to the Cooper minima. (c) Partial cross sections  $\sigma_{\ell 0}$ : solid line with + sign, total cross section  $\sigma_\sigma$ ; thin and thick, solid lines,  $\sigma_{00}$  and  $\sigma_{10}$ ; thin and thick dashed lines,  $\sigma_{20}$  and  $\sigma_{30}$ ; thin and thick dotted-dashed lines,  $\sigma_{40}$  and  $\sigma_{50}$ ; thin and thick double-dotted-dashed lines,  $\sigma_{60}$  and  $\sigma_{70}$ . The vertical dashed lines indicate the position of the Cooper minima in each partial cross sections.

there are Cooper minima evenly separated in the  $\sigma_{\ell 0}$  partial cross sections. We also performed calculations for a  $1s\sigma$  initial state at an internuclear distance  $R=1.5$  a.u. to compare with previous calculations made with a different method by Brosolo *et al.* [23]. We find excellent agreement in the photoelectron momentum range where both calculations overlap and no oscillation in  $\beta$ ,  $\sigma_\sigma$ , and total cross sections.

As a further comparison we now consider the photoionization process of  $\text{HeH}^{2+}$  in the  $2p\sigma$  initial state, which is the lowest electronic attractive state showing a shallow minimum at internuclear distance  $R=3.9$  a.u. [24]. This initial state has nodes and thus, following from the analysis for HCl by Thiel [20], it can be expected that both the  $\beta$  parameter and the total cross section will present structures related to the Cooper minima. We have shown in Sec. III A that for homonuclear one-electron molecules the positions of the Cooper minima are related to the minima in the Young-type periodic oscillations of  $\beta$  and  $\sigma_{\text{tot}}$ . It is evident therefore that the case of  $\text{HeH}^{2+}$  ( $2p\sigma$ ) photoionization must be somehow different since Young-type periodic oscillations are not expected for this asymmetric molecular ion. The results are shown in Fig. 6(a), and we indeed find structures in  $\beta$ . Figure 6(c) presents the contributions from odd and even partial cross sections, which present Cooper minima. Interestingly, the sum  $\sigma_\sigma$  (solid line with + sign) of all the partial cross sections displays oscillations. Moreover, the minima in the

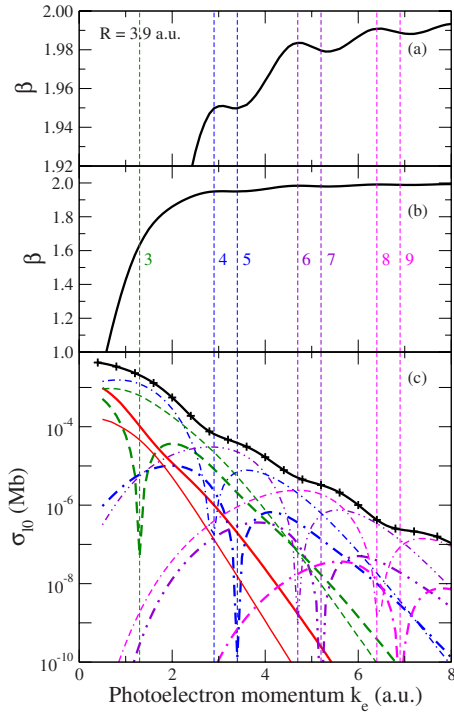


FIG. 6. (Color online) Same as Fig. 5 but for photoionization of  $\text{HeH}^{2+}$  in the  $2p\sigma$  initial state with  $R=3.9$  a.u. The vertical dashed lines indicate the positions of the Cooper minima in each partial cross section.

oscillations appear close to the positions of the Cooper minima for the odd partial waves and the maxima to the positions of the Cooper minima for the even partial waves. The important feature is that, contrary to all previous cases, the value  $k_e(\ell+1)-k_e(\ell)$ , which gives the frequency of the oscillation, is not constant. In fact there are two frequencies, one given by the interval between the Cooper minima of the same symmetry (even or odd) and the other given by the interval between Cooper minima of different symmetry (even-odd). Therefore the oscillations are not periodic so that there is no coherence in the emission from the two centers. It results that only in the case of one-electron homonuclear molecules do the Cooper minima produce the periodic oscillatory behavior predicted by Cohen and Fano which corresponds to Young-type coherent electron emission.

### C. Comparison between photon- and ion-impact-induced ionization

In Secs. III A and III B the connection between the presence of Cooper minima and the oscillatory behavior of the asymmetry parameter and cross sections for photoionization of a one-electron homonuclear target ( $\text{H}_2^+$ ) was established. One can expect that the same features occur in collisions between fast charged particles and  $\text{H}_2^+$ . Indeed, the electron emission process is dominated by a dipolar interaction at high impact energies and thus the connection between photon and charged-particle ionization can be made formally (see [25] for a detailed discussion of this topic).

For charged-particle impact, the process occurs at different impact parameters and all of these contributions have to

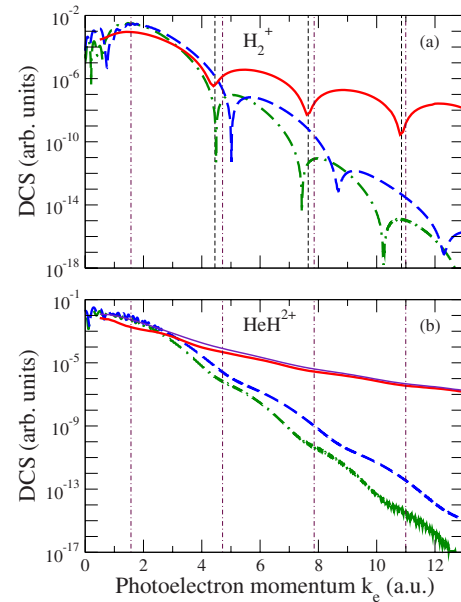


FIG. 7. (Color online) (a) Differential cross section for ionization of  $\text{H}_2^+$  ( $R=2$  a.u.) with the polarization and internuclear vectors in the same direction ( $\Theta_R=0^\circ$ ). Solid line, emission by photon impact; dashed line (dotted-dashed line), emission in the forward (backward) direction by proton impact with projectile velocity  $v=50$  a.u. (b) Same as (a) but for ionization of  $\text{HeH}^{2+}$  ( $R=2$  a.u.). The vertical dashed lines indicate the positions of the minima in the photoionization cross sections and the vertical dotted-dashed lines the Young-type minima as given by Eq. (10).

be summed up. This procedure, which can also be performed in the transverse momentum transfer representation, may somewhat smear out the oscillations [26]. Since we have already shown that the periodic oscillations in  $\beta$  and  $\sigma_{\text{tot}}$  are quite small, we present in this section differential results for a given geometry to avoid any averaging procedure: we consider a geometrical arrangement in which the outgoing electron momentum, the molecular orientation, and the polarization vector are parallel ( $\Theta_R=0^\circ$ ). This corresponds to evaluating the differential cross section (DCS) [cf. Eq. (1)] for forward ( $\theta=\theta_e=0$ ) and backward emission ( $\theta=\theta_e=\pi$ ). We compare our calculations for photoionization with results for ion-impact ionization obtained employing the one-dimensional (1D) nonperturbative time-dependent approach presented by Sisourat *et al.* [27].

In Fig. 7(a) we show the DCS for  $\text{H}_2^+$ , with  $R=2$  a.u., as a function of the electron momentum. This figure shows that both spectra have the same features with deep minima [28], suggesting that independently of the projectile (photon, ion) these minima are produced by the same mechanism. For ion impact they were analyzed by Sisourat *et al.* [27] in the frame of Young-type interferences and predicted to appear when  $k_e$  and  $R$  satisfy the relation

$$k_e R \cos \theta = (2n + 1)\pi. \quad (10)$$

We can readily see that the minima in the spectra of Fig. 7(a) are close to the values of the electron momenta for destructive interference:  $k_e = \pi/2, 3\pi/2, 5\pi/2, 7\pi/2, \dots$  (indicated

by the vertical dotted-dashed lines), except for the first one which does not appear. For ion-induced ionization the difference between forward and backward electron emission was interpreted by Sisourat *et al.* as a consequence of the delay in the ionization of each nucleus due to the finite velocity of the projectile. This effect is absent for photoionization so that there is a complete symmetry between the forward and backward directions. Thus the minima for photon impact appear in the middle of the minima for the ion-impact case.

Another way to interpret the minima in the electron emission is through the Cooper minima. As was noted before, for parallel alignment only  $\sigma \rightarrow \sigma$  transitions can occur. Therefore the sum in Eq. (2) includes only  $m=0$  and each term becomes equal to zero for a specific  $k_e$  value corresponding to the Cooper minimum of the specific matrix element  $M_{\ell 0}$ . Finally, when all terms in the expansion are summed up the DCSs do not drop exactly to zero but present broad minima [indicated by the vertical dashed lines in Fig. 7(a)] for values close to the Cooper minima. This interpretation allows us to understand also why there is no minimum for  $k_e = \pi/2$ . As was shown in Fig. 1(c) the  $\ell=1$  partial cross section has no Cooper minima: Della Picca *et al.* [11] showed that this occurs because this Cooper minimum should appear below threshold. Therefore neither the photon- nor ion-impact-induced spectra shows oscillations corresponding to  $\ell=1$  [ $n=0$  in Eq. (10)].

As was shown in Sec. III B, the correlation between Cooper minima and Young-type interferences only appears for homonuclear molecules and thus we can expect that for the  $\text{HeH}^{2+}$  molecule the destructive interference disappears for ion impact too. We present in Fig. 7(b) the spectra for this molecular ion. Due to the asymmetry of the molecule we consider the two possible geometrical configurations with the He nuclei to the left and to the right of the H nuclei. The results presented in the figure are the average over these two geometries. We can see that there are no clear minima, supporting the idea that the coherent emission from both centers is now strongly weakened since the two slits are different. We note that this behavior is independent of the averaging as the same result appears for each geometrical arrangement. The only difference is that contrary to the homonuclear case there is a very small difference between forward and back-

ward emission which could be observed at small values of photoelectron momentum. This is due to the broken symmetry resulting from the different charges of the nuclei in the molecule. As expected, the cross section for photoelectron emission is always smaller in the direction of the He nuclei due to the larger Coulomb attraction. At very large photoelectron momentum the cross sections for forward and backward emission are equal because the fast electron experiences the potential in the united atom limit which is equal in both cases. However, for ion-induced ionization, the two cross sections are different due to the asymmetry introduced by the positively charged projectile favoring electron emission in the forward direction [29].

#### IV. CONCLUSIONS

Total, partial, and differential photoionization cross sections, calculated using exact bound initial and continuum final states, are presented for one-electron homonuclear  $\text{H}_2^+$  and heteronuclear  $\text{HeH}^{2+}$  diatomic molecular targets. We find a clear periodic oscillation of the asymmetry parameter  $\beta$  in the case of  $\text{H}_2^+$ , while this feature is absent for  $\text{HeH}^{2+}$ . We show that these oscillations are related to the presence of Cooper minima in the partial cross sections and could be observed experimentally in the ratios of the photoionization total cross section for  $\text{H}_2^+$  with the ones for the atomic target. We relate these modulations to coherent electron emission since for homonuclear targets the position of the minima in the oscillations can be exactly predicted by a simple criterion (depending only on the value of the internuclear distance) related to Young double-slit destructive interference effects. As expected, these periodic structures disappear for heteronuclear molecules. Finally, we compare the photoionization spectra with ion-impact-induced electron emission cross sections from the same molecular targets: these results are very similar with respect to the presence of the minima and again support the interpretation of their origin to Young-type interference effects. In summary, we have shown that the interpretations of periodic structures appearing in electron emission spectra for one-electron homonuclear molecular targets in terms of either Cooper minima or Young-type interference effects are equivalent.

- 
- [1] N. Stolterfoht *et al.*, Phys. Rev. Lett. **87**, 023201 (2001).  
 [2] M. E. Galassi, R. D. Rivarola, P. D. Fainstein, and N. Stolterfoht, Phys. Rev. A **66**, 052705 (2002); M. E. Galassi, R. D. Rivarola, and P. D. Fainstein, *ibid.* **70**, 032721 (2004).  
 [3] L. Nagy, L. Kocbach, K. Póra, and J. P. Hansen, J. Phys. B **35**, L453 (2002).  
 [4] C. R. Stia, O. A. Fojón, P. F. Weck, J. Hanssen, and R. D. Rivarola, J. Phys. B **36**, L257 (2003).  
 [5] O. Kamalou, J.-Y. Chesnel, D. Martina, F. Frémont, J. Hanssen, C. R. Stia, O. A. Fojón, and R. D. Rivarola, Phys. Rev. A **71**, 010702(R) (2005).  
 [6] O. A. Fojón, J. Fernández, A. Palacios, R. D. Rivarola, and F. Martín, J. Phys. B **37**, 3035 (2004).  
 [7] H. D. Cohen and U. Fano, Phys. Rev. **150**, 30 (1966).  
 [8] O. A. Fojón, A. Palacios, J. Fernández, R. D. Rivarola, and F. Martín, Phys. Lett. A **350**, 371 (2006).  
 [9] S. K. Semenov, N. A. Cherepkov, M. Matsumoto, T. Hatamoto, X.-J. Liu, G. Prümper, T. Tanaka, M. Hoshino, H. Tanaka, F. Gel'mukhanov, and K. Ueda, J. Phys. B **39**, L261 (2006).  
 [10] X.-J. Liu, N. A. Cherepkov, S. K. Semenov, V. Kimberg, F. Gel'mukhanov, G. Prümper, T. Lischke, T. Tanaka, M. Hoshino, H. Tanaka, and K. Ueda, J. Phys. B **39**, 4801 (2006).  
 [11] R. Della Picca, P. D. Fainstein, M. L. Martiarena, and A. Dubois, Phys. Rev. A **77**, 022702 (2008).  
 [12] S. T. Pratt, Rep. Prog. Phys. **58**, 821 (1995).

- [13] D. Rolles *et al.*, *Nature (London)* **437**, 711 (2005).
- [14] S. K. Semenov and N. A. Cherepkov, *J. Phys. B* **36**, 1409 (2003).
- [15] G. Hadinger, M. Aubert-Frécon, and G. Hadinger, *J. Phys. B* **22**, 697 (1989).
- [16] L. I. Ponomarev and L. N. Somov, *J. Comput. Phys.* **20**, 183 (1976).
- [17] J. Rankin and W. R. Thorson, *J. Comput. Phys.* **32**, 437 (1979).
- [18] J. A. Richards and F. P. Larkins, *J. Phys. B* **19**, 1945 (1986).
- [19] J. Fernández, O. Fojón, A. Palacios, and F. Martín, *Phys. Rev. Lett.* **98**, 043005 (2007).
- [20] W. Thiel, *J. Electron Spectrosc. Relat. Phenom.* **34**, 399 (1984).
- [21] T. A. Carlson, M. O. Krause, W. A. Svensson, P. A. Gerard, F. A. Grimm, T. A. Whitley, and B. P. Pullen, *Z. Phys. D: At., Mol. Clusters* **2**, 309 (1986).
- [22] W. Thiel, *Chem. Phys.* **77**, 103 (1983).
- [23] M. Brosolo, P. Decleva, and A. Lisini, *J. Phys. B* **25**, 3345 (1992).
- [24] J. Fernández and F. Martín, *J. Phys. B* **40**, 2471 (2007).
- [25] A. Voitkiv and J. Ullrich, *J. Phys. B* **34**, 4513 (2001).
- [26] G. Laurent, P. D. Fainstein, M. E. Galassi, R. D. Rivarola, L. Adoui, and A. Cassimi, *J. Phys. B* **35**, L495 (2002).
- [27] N. Sisourat, J. Caillat, A. Dubois, and P. D. Fainstein, *Phys. Rev. A* **76**, 012718 (2007).
- [28] The different decay of the cross sections for the two processes is related to the 1D description of the collision system. To put the photon- and ion-impact ionization cross sections on the same scale the latter were multiplied by  $10^6$ .
- [29] P. D. Fainstein, V. H. Ponce, and R. D. Rivarola, *J. Phys. B* **24**, 3091 (1991).